Malaysian Journal of Analytical Sciences (MJAS) Published by Malaysian Analytical Sciences Society



OPTIMIZATION OF DIFFERENT PARAMETERS IN THE SYNTHESIS OF BISPHENOL A IMPRINTED POLYMER VIA PRECIPITATION POLYMERIZATION FOR BISPHENOL A ADSORPTION

(Pengoptimuman Parameter yang Berbeza dalam Sintesis Polimer Tercetak Bisfenol A Melalui Pempolimeran Pemendakan bagi Penjerapan Bisfenol A)

Tan Nee Nee, Noorhidayah Ishak*, Azalina Mohamed Nasir, Nur Zatul 'Iffah Zakaria, Nur Munirah Rohaizad

Faculty of Chemical Engineering Technology, Universiti Malaysia Perlis. Sungai Chuchuh, 02100 Padang Besar, Perlis, Malaysia

*Corresponding author: noorhidayah@unimap.edu.my

Received: 27 September 2021; Accepted: 12 November 2021; Published: xx December 2021

Abstract

Molecularly imprinted polymer (MIP) is used to synthesize receptors and is highly recognized against target molecules. The purpose of the study is to prepare bisphenol A (BPA) imprinted polymer that can be used to adsorb BPA molecules. The MIP was prepared by precipitation polymerization using BPA as a template, methacrylic acid (MAA) as a functional monomer, ethylene glycol dimethacrylate (EGDMA) as a crosslinker, acetonitrile as a solvent, and 1,1'-azobis(cyclohexanecarbonitrile) (AIBN) as an initiator by heating in an oil bath at 60 °C for 20 hours. The influence of several parameters (i.e., the ratio of monomer-template, the amount of crosslinker, and the amount of solvent) on the recognition capability of BPA MIP was investigated using response surface methodology (RSM). The optimal conditions of BPA synthesis are 3 mmol of monomer, 30 mmol of crosslinker, and 35 mL of solvent, which achieved an adsorption capacity of 78.111 mg/g. The MIP and non-imprinted polymer (NIP) were characterized using Fourier transform infrared (FTIR) spectroscopy and scanning electron microscopy (SEM). The MIP shows higher selectivity towards BPA compared to other analogs. In conclusion, the particles of imprinted polymer have a great potential in the adsorption of BPA.

Keywords: bisphenol imprinted polymer, response surface methodology, imprinted polymer characterization

Abstrak

Polimer molekul tercetak (MIP) digunakan untuk mensintesis reseptor dan mempunyai pengecaman yang sangat tinggi terhadap molekul sasaran. Tujuan kajian ini adalah untuk menyediakan polimer yang dicetak bisfenol A (BPA) yang boleh digunakan untuk menentukan keupayaan penjerapan terhadap molekul BPA. MIP disediakan dengan pempolimeran pemendakan menggunakan BPA sebagai templat, asid metakrilik (MAA) sebagai monomer berfungsi, etilena glikol dimetakrilat (EGDMA) sebagai agen penyilangan, asetonitril sebagai pelarut, dan 1,1 azobis (sikloheksanakarbonitril) (AIBN) sebagai pemula. Pempolimeran pemendakan dilakukan dengan pemanasan dalam rendaman minyak pada 60 °C selama 20 jam. Pengaruh parameter berikut telah disiasat (nisbah monomer-templat, jumlah agen penyilangan, dan jumlah pelarut yang digunakan). Kaedah matematik iaitu kaedah tindak balas permukaan (RSM) mengoptimumkan parameter ini untuk meningkatkan keupayaan pengesanan BPA MIP. Hasil yang diperoleh daripada RSM menunjukkan keadaan optimum 3 mmol jumlah monomer, 30 mmol jumlah agen penyilangan, dan 35

mL jumlah pelarut yang digunakan dengan kapasiti penjerapan sebanyak 78.111 mg/g. MIP juga mempunyai pemilihan yang lebih tinggi terhadap BPA berbanding dengan analog lain. Kesimpulannya, zarah polimer tercetak menunjukkan potensi yang baik terhadap penjerapan cecair BPA.

Kata kunci: polimer bisfenol tercetak, kaedah tindak balas permukaan, pencirian polimer tercetak

Introduction

The chemical name for bisphenol A (BPA) is 2,2-bis(4-hydroxyphenyl)propane [1]. Since the 1940s and 1950s, BPA has been used in the plastic industry. BPA can be classified as an endocrine-disrupting chemical commonly used to manufacture polycarbonate plastics, polysulfones, and epoxy resins. BPA leaches easily from polycarbonate food and drink containers, can interfere with hormone systems, and has an adverse effect on the environment [2]. Furthermore, BPA can cause various health issues, including breast cancer, obesity, and fertility problems in men and women [3].

Three types of processes that can remove BPA from water or wastewater are microbiological, chemical, and physical processes [4]. A microbiological process uses bacteria for the removal of endocrine-disrupting compounds [5]. Meanwhile, advanced oxidation process is a chemical process that uses ozone and UV radiation. Reverse osmosis, nanofiltration, and adsorption are examples of physical processes [4]. Molecular imprinting technique has been proposed to remove BPA in an aqueous solution due to its reusability and low cost.

Molecularly imprinted polymer (MIP) can identify any target molecule specifically, and it is a type of synthetic polymer. The mixture of template molecules, functional monomers, crosslink monomers, and initiators is polymerized to obtain the imprinted polymer. During polymerization, the complexes are heated, forming a rigid polymer structure consisting of template molecules, functional monomers, and crosslinkers. A high degree of cross-linking maintains the polymer matrix's form after removing the template molecule from the polymer matrix [6,7]. The non-imprinted polymer (NIP) that is commonly synthesized with MIP will act as a control so that the selectivity of the MIP can be analyzed by comparing it with the binding capacity data of NIP. The NIP preparation will follow all the

polymerization processes of MIP, except that the template molecule is absent during polymerization.

Bulk polymerization is a conventional method widely used to synthesize MIP. However, this method suffers from the irregular shape of polymer and non-uniform particle size distribution due to the crushing processes. Therefore, the resultant polymers need to be sieved to obtain the desired particle size. The sieving process is time-consuming, and crushing can destruct the cavity of the template, thus affecting the polymer's performance. Therefore, precipitation polymerization has been proposed to overcome the disadvantages of bulk polymerization. MIP synthesis using precipitation polymerization employs a similar method as bulk polymerization. However, the amount of porogen used is higher than bulk polymerization. This method can produce polymer particles without the crushing process, free from additional surfactants or stabilizers. The amount of porogen, crosslinker, template, and monomer is significant to obtain a highly sensitive and selective polymer [8].

Design-Expert version 11 has been used to evaluate experimental responses using response surface methodology (RSM) by carrying out experiments and numerical modeling. It is a faster and cheaper way of collecting research findings than the classical onefactor-at-a-time (OFAT) method or full-factorial experiments. RSM also provides a model equation for the response parameter and optimizes process variables [9]. Several factors will affect the characteristics of the imprinted polymers. One of the factors is the amount of porogenic solvent used, which will affect the monomertemplate interactions [10]. In addition, different ratios of template molecule to functional monomer will affect the complexity of the template [11]. Lastly, the amount of crosslinkers used will affect the stability of the recognition sites [10]. All of these factors are very

important during the preparation of imprinted polymer particles. However, not much study has been done to optimize these important parameters. Throughout this research, the interaction of the parameters and their effects on the binding capacity were studied. The parameters of the polymerization process (i.e., the amount of monomer, crosslinker, and porogenic solvent) were chosen and optimized using RSM coupled with central composite design (CCD) to produce MIPs with optimum recognition to adsorb BPA molecules. This preliminary study will create a paradigm for future studies in the development of receptors in supramolecular chemistry.

Materials and Methods

Raw materials

Bisphenol A (BPA), methacrylic acid (MAA), acetonitrile, ethylene glycol dimethacrylate (EGDMA), acetic acid, diphenylamine, diphenyl phosphate, hydroquinone, and diethylstilbestrol were purchased from Sigma-Aldrich, whereas 1,1'-azobis (cyclohexanecarbonitrile) (AIBN) was acquired from Acros Organics.

Preparation of MIP and NIP

The preparation of BPA for MIP was conducted under different conditions. One mmol BPA (template) and MAA (functional monomer), acetonitrile, EGDMA (crosslinker), and 50 mg AIBN (initiator) were added to a bottle. Next, the mixture was purged for 10 min with a gentle nitrogen flow [12]. The bottle was closed immediately. Then, the mixture was sonicated for 15 min. The solution was polymerized in a 60 °C oil bath for 20 h. After that, the polymer particles were washed with methanol to remove unreacted reagents. Then, the template molecule was repeatedly extracted after polymerization using a methanol-acetic acid solution (9:1 v/v) until the ultraviolet-visible (UV-Vis) spectrophotometer did not detect BPA from the washing solvent at 278 nm [13]. Next, the extracted particles were washed repeatedly with methanol to remove residual acetic acid. This washing step was done by shaking the particles at 130 rpm for 2 h. Lastly, the MIP was dried in an oven at 50 °C for 24 h [13]. As a control, the NIP was synthesized and treated in the same way,

except that the template molecule was absent in the polymerization stage.

Preparation of MIP and NIP for BPA Adsorption

Approximately 10 mg of the MIP or NIP was placed in a centrifuge tube and 25 mL of an 80 mg/L BPA solution. The mixed solution was shaken at 150 rpm for 2 h at constant temperature in a centrifuge tube. Then, the solution was separated centrifugally at 4,000 rpm for 10 min. After centrifuging, the supernatant solution was decanted and filtered using a 0.20 µm syringe filter. UV-Vis spectrophotometers were used to measure the solution concentration changes with BPA at 278 nm [14]. All testing was conducted in triplicate, and the average data values were used to ensure the accuracy of the data collected. The adsorption capacity of BPA (Q) was calculated using Equation 1 [15]:

Adsorption Capacity,
$$Q = \frac{(C_i - C_f) V}{m}$$
 (1)

where C_i is initial solution concentration (mg/L), C_f is final solution concentration (mg/L), V is volume of the solution (mL) and m is mass of dried polymer (mg).

Optimization of the preparation conditions of MIP for BPA removal

The experimental design was conducted with the help of RSM in Design-Expert version 11 to optimize the adsorption capacity. A CCD was utilized to study the response pattern and determine the optimum combination of variables. A CCD-based RSM was used to optimize the parameters selected for BPA removal, which were different ratios of monomer-template, amount of crosslinker, and amount of solvent. The design was used to investigate the combined effect of three independent parameters, and 20 sets of experiments were carried out. The range to optimize the three parameters is shown in Table 1.

Characterization of MIP and NIP

The surface morphology of MIP and NIP was analyzed using SEM. Before measuring in SEM, the sample was first mounted on aluminum stubs using double-sided adhesive tape and sputtered with a thin platinum film. The functional groups of MAA were characterized using attenuated total reflectance-Fourier transform infrared

Tan et al: OPTIMIZATION OF DIFFERENT PARAMETERS IN THE SYNTHESIS OF BISPHENOL A IMPRINTED POLYMER VIA PRECIPITATION POLYMERIZATION FOR BISPHENOL A ADSORPTION

(ATR-FTIR) spectroscopy, while the MIP, NIP, and BPA were characterized using FTIR spectroscopy. A potassium bromide (KBr) pellet is usually used for the analysis of a powdered sample. In this study, KBr pellet samples were scanned in the wavenumber range of 4000–400 cm⁻¹ with a resolution of 4 cm⁻¹ [16]. The FTIR spectrum was recorded and analyzed.

Selectivity Experiment on BPA

In order to prove the specific selectivity of the optimized MIP and NIP to BPA, hydroquinone, diethylstilbestrol, diphenylamine, and diphenyl phosphate were chosen as analogs. Firstly, the standard calibration curve for each analog was prepared with the concentration of 20, 40, 60, 80, and 100 mg/L. The MIP and NIP (10 mg) were first dispersed respectively in a mixture solution containing BPA or other different analogs (80 mg/L, 25 mL) and shaken at 25 °C and 150 rpm for 2 h. After adsorption, the mixture solution was separated by centrifuge at 4,000 rpm for 10 min, and the supernatant

was de___ited and filtered using a 0.20 μ m syringe filter. The supernatant was measured by a UV spectrometer with each of the specific wavelengths. The average values of the data were determined. The adsorbed amount of BPA or other analogs was calculated according to Equation 1. Meanwhile, the imprinting factor (α_{ana}) and selectivity factor (β) of MIP and NIP were calculated using Equation 2 and 3, respectively:

Imprinting Factor
$$(\alpha_{ana}) = \frac{Q_{MIP}}{Q_{NIP}}$$
 (2)

Selectivity Factor (
$$\beta$$
) = $\frac{\alpha_{tem}}{\alpha_{ana}}$ (3)

where Q_{MIP} and Q_{NIP} are the adsorption capacity of the template or analog molecule on MIP and NIP, respectively, and α_{tem} and α_{ana} are the imprinting factor for the template molecule and analog, respectively [15].

Table 1. Experimental range and levels of the chosen parameters

Parameters	Code	Range and Levels		
		-1	0	1
Amount of monomer, MAA (mmol)	A	2	3	4
Amount of crosslinker, EDGMA (mmol)	В	20	30	40
Amount of solvent, acetonitrile (mL)	C	20	35	50

Results and Discussion

Design response surface methodology for optimum polymerization parameters

Table 2 shows the sequential model sum of squares for BPA adsorption capacity. The models available are linear, 2FI, quadratic, and cubic. The greater *F*-value and the lower *p*-value suggest that the model is highly significant and shown to be good [17]. In this case, the recommended source is quadratic vs 2FI with the sum of squares of 5,233.23 and an *F*-value of 56.40. However, the model is also significant because the *p*-value is smaller than 0.0001.

Analysis of variance for the quadratic model

Table 3 shows an analysis of variance (ANOVA) for the response surface quadratic model. The model is significant, as the F-value is 33.22 and the p-value is smaller than 0.0001. This implies that the chance of the model F-value occurring due to noise is negligible [18]. In this case, the linear coefficients (A, C), interaction coefficients (AB, AC, BC), and quadratic coefficients (A², B², C²) are significant. Furthermore, p-values of less than 0.05 strongly support their significant contribution to adsorption capacity [19]. In contrast, the amount of crosslinker does not significantly affect adsorption capacity as it has a low F-value of 1.05 and a high p-value of 0.3291.

In addition, the coefficient of determination (R²) value is close to unity (i.e., 0.9676). According to Zhou [20], in order to verify the favorable consistency between actual data and theoretical prediction, the R² value should be at least 0.800. From Table 3, the adjusted R² value is 0.9385. Therefore, it is confirmed that the model is very significant, indicating a good agreement between the experimental and predicted values. Owolabi and coworkers stated that the adjusted R² and predicted R² values must be in good agreement within 20% [9]. In this study, this requirement is met with a predicted R² value of 0.7452. These values represent good adsorption capacity of MIP towards BPA. The adequate precision ratio of 15.6517 indicates a suitable signal-to-noise

ratio. The ratio was greater than 4; thus, the quadratic model could navigate the design space and find the optimal conditions for adsorption capacity [18].

The application of RSM yields the quadratic regression equation as indicated in Equation 4, representing an empirical relationship between adsorption capacity and process variables in coded values, where A is the amount of monomer, b is the amount of crosslinker, and C is the amount of solvent. A positive symbol in the equation denotes a synergistic effect, whereas a negative symbol represents an antagonistic effect [21].

Table 2. A sequential model sum of squares for BPA adsorption capacity

Source	Sum of Squares	df	Mean Square	F-value	<i>p</i> -value	
Mean vs Total	63,694.01	1	63,694.01			
Linear vs Mean	2,790.02	3	930.01	2.20	0.1279	
2FI vs Linear	1,224.26	3	408.09	0.9572	0.4420	
Quadratic vs 2FI	5,233.23	3	1,744.41	56.40	< 0.0001	Suggested
Cubic vs Quadratic	283.41	4	70.85	16.42	0.0022	Aliased
Residual	25.89	6	4.31			
Total	73,250.82	20	3,662.54			

Table 3. Analysis of variance for the response surface quadratic model

Source	Sum of Squares	df	Mean Square	F- value	<i>p</i> -value
Model	9,247.52	9	1,027.50	33.22	< 0.0001
A-Amount of monomer	1131.95	1	1,131.95	36.60	0.0001
B-Amount of crosslinker	32.55	1	32.55	1.05	0.3291
C-Amount of solvent	1,625.52	1	1,625.52	52.55	< 0.0001
AB	220.53	1	220.53	7.13	0.0235
AC	407.31	1	407.31	13.17	0.0046
BC	596.42	1	596.42	19.28	0.0014
A^2	174.20	1	174.20	5.63	0.0391
B^2	540.81	1	540.81	17.48	0.0019
C ²	666.02	1	666.02	21.53	0.0009
Residual	309.30	10	30.93		

Std. dev. = 5.56, C.V. % = 9.85

 $R^2 = 0.9676$, Adj. $R^2 = 0.9385$,

Predicted $R^2 = 0.7452$, Adeq Precision = 15.6517

Adsorption Capacity =
$$75.21 + 10.64A - 1.80B + 12.75C + 5.25AB + 7.14AC - 8.63BC - 7.96A^2 - 14.02B^2 - 15.56C^2$$
 (4)

Diagnostic study

The validity of the derived equation is discussed in a series of graphical diagnoses. Figure 1(a) shows that the data points are scattered along the straight line of a typical residual graph, indicating that the data points form a normal distribution [21]. Another confirmation is the residual plot versus the predicted response (Figure 1(b)), where the random pattern in the residual plot versus the predicted response indicates that the model is satisfactory and also does not interfere with the independence or constant variance assumption [18]. On the other hand, it has been inferred that from the externally studentized residual plot versus the run number in Figure 1(c), not all data points deviate far from the values predicted [22]. The data points in the predicted versus actual plot in Figure 1(d) are scattered along a straight line, indicating that the experimental and predicted response values are correctly associated [23]. As a result, the derived quadratic response model (Equation 4) reified to be a reliable model representing ads tion capacity.

Analysis of response surface

The purpose of this analysis is to optimize the parameters for BPA adsorption capacity during polymerization. Therefore, this section analyzes the relationship of the three parameters (i.e., the amount of monomer, crosslinker, and solvent) and their respective optimal condition range. There are 20 runs experiments with different operating conditions. Table 4 shows the experimental design matrix with coded factors. A three-dimensional response surface was produced to determine the relationship between the variables and the optimal state of each factor for maximum adsorption capacity. Figure 2(a) presents the effect of the amount of monomer and crosslinker on the adsorption capacity of MIPs. It can be seen that there is higher adsorption capacity when the amount of monomer and crosslinker is 3 mmol and 30 mmol, respectively. However, when the amount of monomer and crosslinker exceeded these values, it is still in an optimal condition, but the adsorption capacity

decreased. The decreasing adsorption capacity is due to the excess amount of monomer, which leads to the creation of non-selective binding sites. In contrast, an extremely high crosslinker amount reduces the number of recognition sites per MIPs unit mass [24]. Therefore, only the appropriate amount of monomer and crosslinker could lead to the maximum adsorption capacity.

Figure 2 (b) represents the effect of monomer and solvent amount on the adsorption capacity of MIPs. The adsorption capacity increased as the amount of monomer and solvent increased. An increased amount of monomer will give a strong interaction between the functional monomer and the template [9]. The additional amount of solvent favors the formation of polar interaction between the monomer and the template [15]. However, it can be seen that the adsorption capacity decreased as the amount of monomer and solvent reduced to below 3 mmol and 35 mL, respectively. It could be explained that the small amount of MAA could not mix sufficiently with BPA molecules, thus minimizing specific recognition sites. In contrast, less solvent can cause the polymer to precipitate early [12, 15]. Thus, the maximum adsorption efficiency could only be achieved through the appropriate amount of monomer and solvent.

Figure 2(c) shows the effect of the amount of crosslinker and solvent on the adsorption capacity of MIPs. From the figure, the maximum adsorption capacity could be achieved when the crosslinker amount is 30 mmol and the solvent amount is 35 mL. However, when the amount of crosslinker and solvent is less than 30 mmol and 35 mL, respectively, it is still in optimum condition, but the adsorption capacity decreased. The reduction is because a low crosslinker amount reduces structural stability, whereas less solvent can lead to early polymer precipitation [12, 13]. Nevertheless, the maximum adsorption capacity could be reached only by the appropriate amount of crosslinker and solvent. In conclusion, this model predicted that the amount of

monomer, crosslinker, and solvent of 3 mmol, 30 mmol, and 35 mL, respectively, as the optimum conditions to achieve the besponse of adsorption capacity towards BPA, which was 78.11 mg/g.

FTIR analysis

In order to characterize the MIP and NIP, the functional groups of BPAs, MAA, MIP, and NIP were analyzed. The FTIR spectra of these four samples are shown in Figure 3 and Table 5. From the observation, BPA has a broad peak at 3325 cm⁻¹, representing O-H stretching. Meanwhile, the peak at 2966 cm⁻¹ shows sp³ C-H stretching and the peak at 823 cm⁻¹ indicates benzene derivative. Next, the stretching frequency of C=O for MIP and NIP at 1726 cm⁻¹ is due to the presence of a poly(EGDMA) backbone. In MAA, the spectrum band at 1694 cm⁻¹ refers to C=O conjugated carbonyl stretching [25]. This band overlaps with the C=O of EGDMA around 1726 cm⁻¹ due to the disappearance of the alkene group in MAA after polymerization. The similarity between these MIP and NIP spectra shows that these polymers have a similar backbone. The FTIR spectra of NIP and MIP indicate that the template molecules have been successfully removed from the MIP, whereby no significant peak of BPA is present [26]. Moreover, the band for MIP and NIP at 1156 cm⁻¹ shows strong C-O-C ester stretching. This band indicates EGDMA and MAA copolymerization due to EGDMA characteristics in the FTIR spectrum [27]. The C=O stretch, C-O stretch, and C-O-C stretch at 1726 cm⁻ ¹, 1257 cm⁻¹, and 1156 cm⁻¹, respectively, demonstrate that MIP has been successfully synthesized.

SEM analysis

The changes in the surface morphology of the MIP after the extraction of template and NIP were analyzed using SEM. Figure 4 displays the surface morphology of MIP and NIP at $5{,}000\times$ and $500\times$ magnification. Both polymers show a relatively rough and porous surface. Acetonitrile that functions as a porogen during polymerization contributes to the macroporous structure on the surface of imprinted polymers. Thus, this explains the adsorption behavior of NIP [7]. The size of the polymer particles was recorded between the range of 11 μ m and 65 μ m.

Selectivity studies on BPA

BPA and other four similar structures (diphenylamine, hydroquinone, diphenyl phosphate, diethylstilbestrol) were selected as analogs for selectivity studies. From Table 6, MIP exhibits a higher binding affinity for BPA than other analogs in adsorption capacity due to the selective recognition sites in the MIP [28]. The higher adsorption capacity indicates that the polymer is specifically selective towards BPA and not the other four analogs. Besides, the imprinting factor represents MIP's special recognition, and a high value means that the MIP has a greater recognition and stronger imprinting effect [29]. Table 6 shows that BPA has a high imprinting factor value compared to other analogs.

Moreover, if the selectivity factor value is higher, the MIPs have greater template selectivity and distinguish the template from the analogs more efficiently [29]. For example, diphenylamine has the highest selectivity factor due to a more specific site and can distinguish BPA from other analogs compared to NIP. Thus, MIP has higher selectivity towards BPA compared to other analogs.

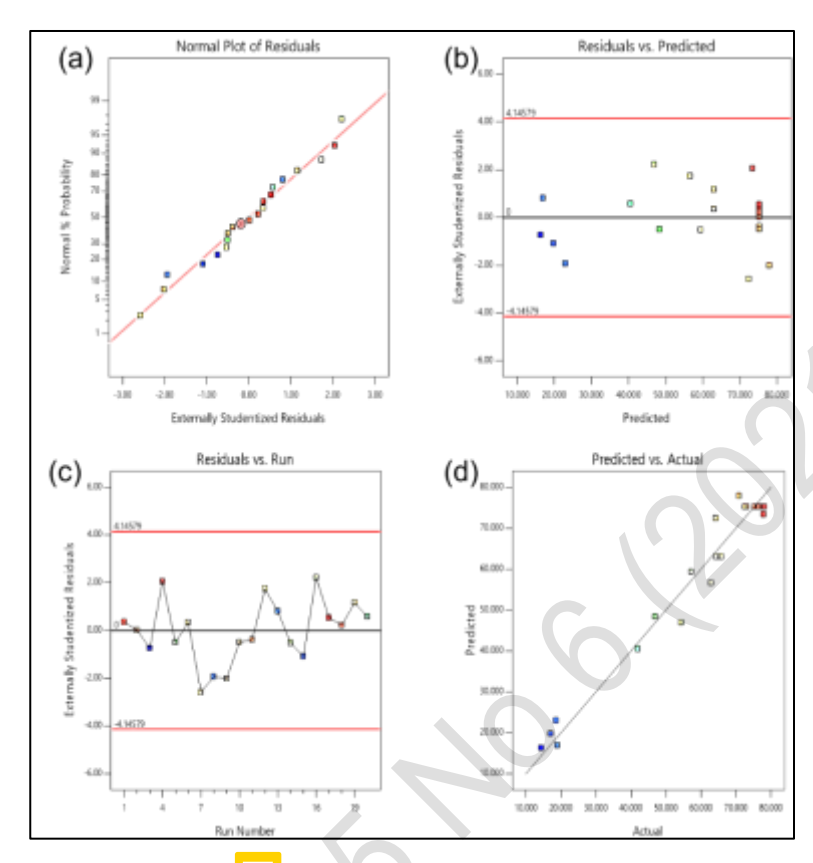


Figure 1. Contextive graphical diagnostics for equation 4

Table 4. Experimental design matrix with coded factors of CCD and response

	Factor 1	Factor 2	Factor 3	Response 1
Run	A: Monomer: Template Ratio (mmol)	B: Amount of Crosslinker (mmol)	C: Amount of Solvent (mL)	Adsorption Capacity (mg/g)
1	3	30	35	77.115
2	3	30	35	75.334
3	4	20	20	14.423
4	4	20	50	77.885
5	2	20	50	47.000
6	3	20	35	64.423
7	3	30	50	64.222
8	2	40	20	18.655
9	4	30	35	70.889
10	3	30	35	72.556
11	3	30	35	73.111
12	2	30	35	62.885

Table 4 (cont'd).	Experimental of	design matrix v	with coded	factors of CCD	and response

	Factor 1	Factor 2	Factor 3	Response 1
Run	A: Monomer: Template Ratio (mmol)	B: Amount of Crosslinker (mmol)	C: Amount of Solvent (mL)	Adsorption Capacity (mg/g)
13	2	40	50	19.038
14	3	40	35	57.222
15	2	20	20	17.115
16	3	30	20	54.345
17	3	30	35	78.111
18	3	30	35	76.445
19	4	40	50	65.889
20	4	40	20	42.000

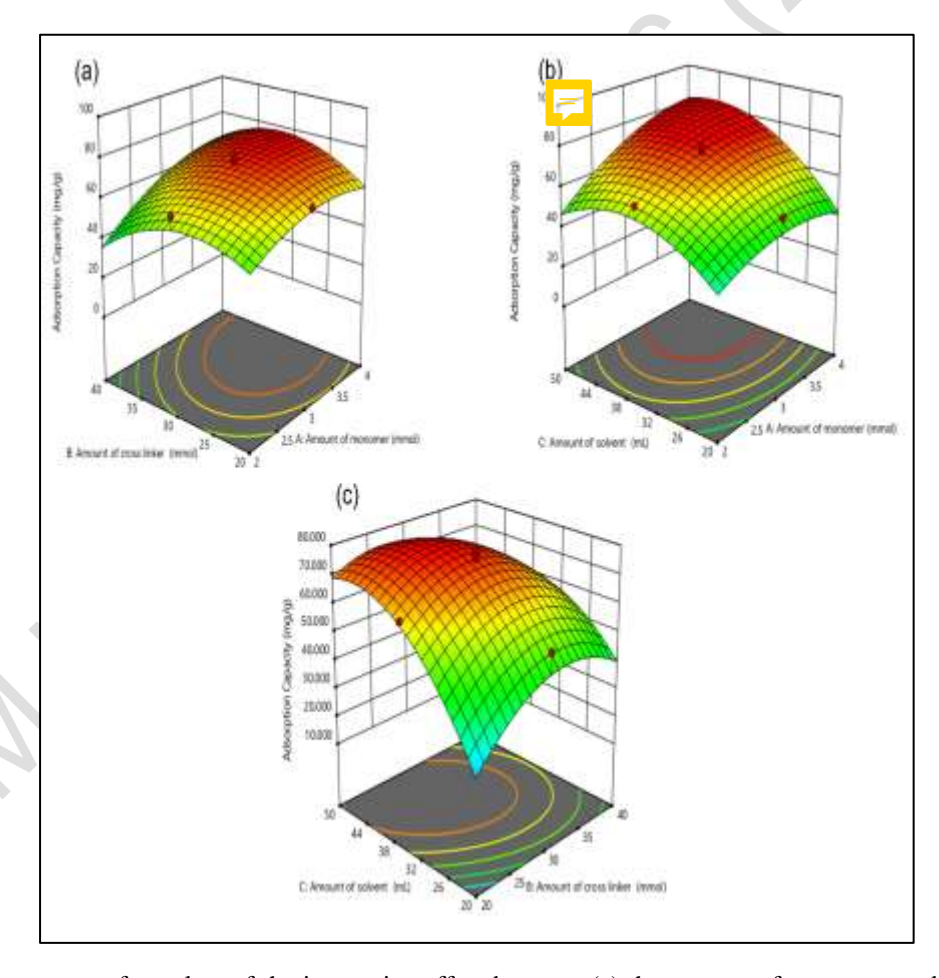


Figure 2. Response surface plots of the interactive effect between (a) the amount of monomer and crosslinker on adsorption capacity, (b) the amount of monomer and solvent on adsorption capacity, and (c) the amount of crosslinker and solvent on adsorption capacity.

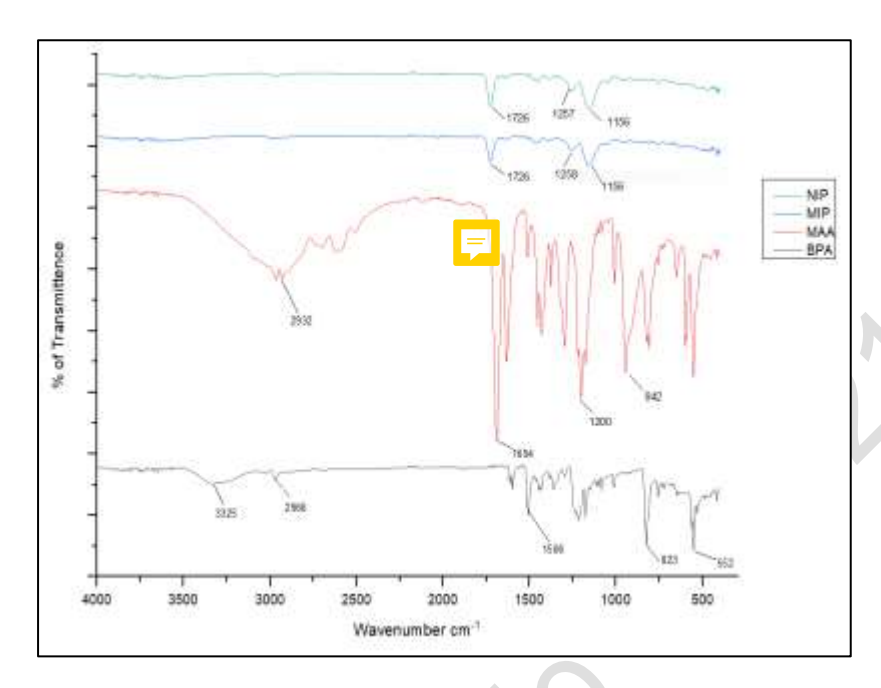


Figure 3. FTIR spectra of BPA, MAA, MIP, and NIP

Table 5. Wavenumber and type of band for MIP/NIP, BPA, and MAA

Type of Material	Wavenumber (cm ⁻¹)	Type of Band
MIP/NIP	1726	C=O stretch
	1257, 1258	C-O stretch
	1156	C-O-C stretch
BPA	3325	O-H stretch
	823	Sp ² C-H band
	2966	Sp ³ C-H stretch
MAA	1694	C=O conjugated carbonyl stretching
	1200	C-O stretch

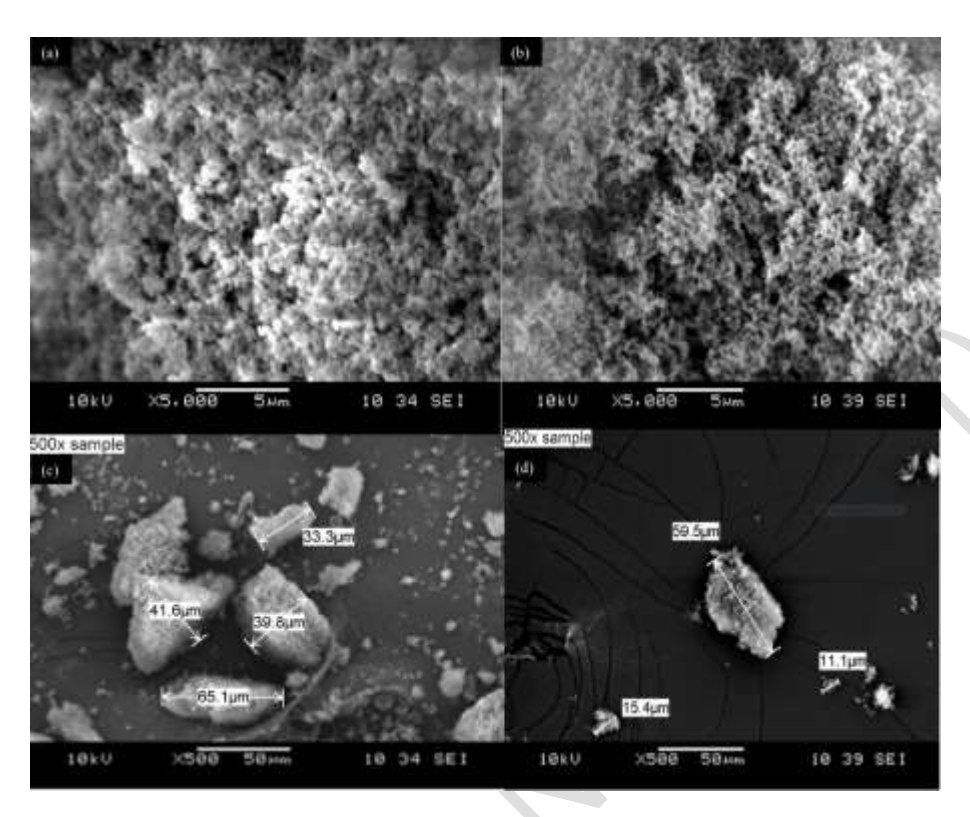


Figure 4. Scanning electron microscopy of MIP

Table 6. The binding capacity, imprinting factor, and selectivity factor of the optimized MIP and NIP

Compound	Binding Capacity (mg/g)		Imprinting	Selectivity
•	MIP NIP		Factor (α)	Factor (β)
BPA	78.111	38.945	2.006	-
Diphenylamine	29.869	28.882	1.034	1.940
Hydroquinone	19.137	18.244	1.049	1.912
Diphenyl Phosphate	57.400	47.400	1.211	1.656
Diethylstilbestrol	40.156	38.5938	1.041	1.928

Conclusion

This study focuses on optimizing the synthesis of BPA imprinted polymer via precipitation polymerization for BPA removal. RSM coupled with CCD was used to evaluate the optimum parameters during polymerization (i.e., different ratios of monomer-template, amount of crosslinker, and amount of solvent used) in terms of adsorption efficiency towards BPA molecules. From the results, the optimum values are 3 mmol of monomer, 30

mmol of crosslinker, and 35 mL of solvent, which achieved the adsorption capacity of 78.111 mg/g. The synthesized BPA imprinted polymer and NIP characteristics were determined by FTIR and SEM analysis. The FTIR analysis indicates no difference between the MIP and NIP spectra because the template molecule has been successfully removed from the MIP. The presence of C=O stretch, C-O stretch, and C-O-C stretch indicates that the MIP has been successfully

synthesized. Based on SEM results, the MIP has a rough and porous surface due to template removal. The MIP also has higher selectivity towards BPA compared to other analogs. This preliminary work reported a satisfactory result of binding capacity and selectivity, highlighting the potential application of BPA imprinted polymer in separation and wastewater treatment. The model developed using RSM coupled with CCD has improved the development of an efficient adsorbent, thus providing a framework for further analysis.

Acknowledgment

The authors would like to thank the Faculty of Engineering Technology, Universiti Malaysia Perlis. The financial support from the Fundamental Research Grant Scheme (FRGS) (FRGS/1/2019/TK05/UNIMAP/03/2) is gratefully acknowledged.

References

- Ya, M. Haohao, L. Jinxia, W. Le, Y. Yueqin, W. Xingde D. Rui, W. Phelisters, W. M. Pavankumar, P. Xinghai, C. and Huizhen, Z. (2019). The adverse health effects of bisphenol A and related toxicity mechanisms. *Environmental Research*, 176: 108575.
- Bayramoglu, G. Arica, M. Y. Liman, G. Celikbicak
 O. and Salih, B. (2016). Removal of bisphenol A
 from aqueous medium using molecularly surface
 imprinted microbeads. *Chemosphere*, 150: 275-84.
- 3. Metz, C. M. (2016). Bisphenol A: Understanding the controversy. *Workplace Health and Safety* 1, 64: 28-36
- 4. Posada A. L. L (2016). Removal of endocrine disrupting compounds from water and wastewater using ecofriendly materials. Thesis of Master Degree, The University of Texas at El Paso.
- Bhatnagar, A. and Anastopoulos, I. (2017). Adsorptive removal of bisphenol A (BPA) from aqueous solution: A review. *Chemosphere*, 168: 885-902.
- 6. Tehila S. Noam, T. and Daniel, M. (2016). Molecularly imprinted polymer particles: Formation, characterization and application. *Colloids and Surfaces A: Physicochemical and Engineering Aspects*, 495: 11-19.

- Sajini T. and Beena M. (2021). A brief overview of molecularly imprinted polymers: Highlighting computational design, nano and photo-responsive imprinting. *Talanta Open*, 4: 100072.
- 8. Ahmed, S. A. D., Alaa, M. A. and Ibrahim, M. E. (2020). Surface-imprinted polymers (SIPs): Advanced materials for bio-recognition. *Journal of Nanotechnology & Advanced Materials*, 8(1): 1-19.
- 9. Owolabi, R. U. Usman, M. A. and Kehinde, A. J. (2018). Modelling and optimization of process variables for the solution polymerization of styrene using response surface methodology. *Journal of King Saud University Engineering Sciences*, 30(1): 22-30.
- Kelvin, F. P. Maretty, E. R. M. Driyanti, R. and Aliya, N. H. (2020). Effect of the molecularly imprinted polymer component ratio on analytical performance. *Chemical Pharmaceutical Bulletin*, 68: 1013-1024.
- 11. Yemiş, F., Alkan, P., Yenigül, B. and Yenigül, M. (2013). Molecularly imprinted polymers and their synthesis by different methods. *Polymers and Polymer Composites*, 21(3): 145-150.
- Zhao, L., Hu, X., Zi, F., Liu, Y., Hu, D., Li, P. and Cheng, H. (2021). Preparation and adsorption properties of Ni(II) ion-imprinted polymers based on synthesized novel functional monomer. *e-Polymers*, 21(1): 590-605.
- Lu, Y., Zhu, Y., Zhang, Y. and Wang, K. (2019).
 Synthesizing vitamin E molecularly imprinted polymers via precipitation polymerization. *Journal of Chemical & Engineering Data*, 64(3): 1045-1050.
- Shahaidah, S. Che K. M. F. and Shareena, M. S. (2014). Characterization of bisphenol A MIP (BPA-MIP) synthesizing. *Applied Sciences*, 14(13): 1455-1459.
- Jin, X. Wang, Y. Bai, W. Zhao, D. Song, X. and Xu, X. (2015). Synthesis and characterization of fomesafen imprinted polymers. *Journal of Macromolecular Science, Part A: Pure and Applied Chemistry*, 52(4): 316-321.

- Amin, S. Damayanti, S. and Ibrahim, S. (2019).
 Synthesis and characterization molecularly imprinted polymers for analysis of dimethylamylamine using acrylamide as monomer functional. *Jurnal Kefarmasian Indonesia*, 8: 76-84.
- 17. Das, B. (2017). Response surface modeling of copper (II) adsorption from aqueous solution onto neem (*Azadirachta indica*) bark powder: Central composite design approach. *Journal of Materials and Environmental Science*, 8(7): 2442-2454.
- 18. Arabzadeh, N. Mohammadi, A. Darwish, M. and Abuzerr, S. (2018). Construction of a TiO₂–Fe₃O₄-decorated molecularly imprinted polymer nanocomposite for tartrazine degradation: Response surface methodology modeling and optimization. *Journal of the Chinese Chemical Society*, 8: 1-10.
- 19. Gholami, H., Arabi, M., Ghaedi, M., Ostovan, A. and Bagheri, A. R. (2019). Column packing elimination in matrix solid phase dispersion by using water compatible magnetic molecularly imprinted polymer for recognition of melamine from milk samples. *Journal of Chromatography A*, 1594: 13-22.
- Zhou, J. Chen, X. H. Pan, S. D. Wang, J. L. Zheng, Y. B. Xu, J. J. Zhao, Y. G. Cai, Z. X. and Jin, M. C. (2019) Contamination status of bisphenol A and its analogues (bisphenol S, F and B) in foodstuffs and the implications for dietary exposure on adult residents in Zhejiang Province. *Food Chemistry*, 294:160-170.
- Priya, M. Sarveishwhary, R. Saw, H. L. Marinah, M. A. and Khalik, W. M. A. W. M. (2021). CO₂effervescent tablet-assisted dispersive liquid-liquid microextraction with central composite design for pre-concentration of acetaminophen drug: Method development, validation and green assessment profile. *Malaysian Journal of Analytical Sciences*, 25(3): 432-445.
- 22. Talib, N. A. A. Salam, F. Yusof, N. A. Alang, A. S. A. and Sulaiman, Y. (2017). Optimization of peak

- current of poly(3,4-ethylenedioxythiophene)/multi-walled carbon nanotube using response surface methodology/central composite design. *RSC Advances*, 7(18): 11101-11110.
- 23. Liu, Y. Liu, F. Ni, L. Meng, M. Meng, X. Zhong, G. and Qiu, J. (2016). A modeling study by response surface methodology (RSM) on Sr(II) ion dynamic adsorption optimization using a novel magnetic ion imprinted polymer. *RSC Advances*, 6(60): 54679-54692.
- 24. Li, G. and Row, K. H. (2018). Recent applications of molecularly imprinted polymers (MIPs) on micro-extraction techniques. *Separation and Purification Reviews*, 47(1): 1-18.
- 25. Lei, X. N. X. Lu, L. Xinan, X. and Yan, L. (2020). Theoretical insight into the interaction between chloramphenicol and functional monomer (methacrylic acid) in molecularly imprinted polymers. *International Journal of Molecular Science*, 21(11): 4139.
- 26. Kia, S. Fazilati, M. Salavati, H. and Bohlooli, S. (2016). Preparation of a novel molecularly imprinted polymer by the sol-gel process for solid phase extraction of vitamin D3. *RSC Advances*, 6(38): 31906-31914.
- Ishak, N. Ahmad, M. N. Nasir, A. M. and Islam, A. K. M. S. (2015). Computational modelling and synthesis of molecular imprinted polymer for recognition of nitrate ion. *Malaysian Journal of Analytical Sciences*, 19(4): 866-873.
- 28. Xie, X. Ma, X. Guo, L. Fan, Y. Zeng, G. Zhang, M. and Li, J. (2019). Novel magnetic multi-templates molecularly imprinted polymer for selective and rapid removal and detection. *Chemical Engineering Journal*. 357: 56-65.
- Yixuan, Z. Yuxiao, C. Ningning, C. Yuyan, Z. Bingyu L. Wei G. Xinhao, S. and Yuezhong, X. (2014). Recyclable removal of bisphenol A from aqueous solution by reduced graphene oxide-magnetic nanoparticles: Adsorption and desorption. *Journal of Colloid and Interface Science*, 421: 85-92.